

CONSTRAINED MULTI-OBJECTIVE SHAPE OPTIMIZATION OF SUPERCONDUCTING RF CAVITIES TO COUNTERACT DANGEROUS HIGHER ORDER MODES

M. Kranjčević*, P. Arbenz, Computer Science Department, ETH Zurich, 8092 Zürich, Switzerland
 A. Adelman, Paul Scherrer Institut (PSI), 5232 Villigen, Switzerland
 S. Gorgi Zadeh, U. van Rienen, University of Rostock, 18059 Rostock, Germany

Abstract

High current storage rings, such as the Z operating mode of the FCC-ee (FCC-ee-Z), require superconducting radio frequency (RF) cavities that are optimized with respect to both the fundamental mode and the dangerous higher order modes (HOMs). In this paper, in order to optimize the shape of the RF cavity, a constrained multi-objective optimization problem is solved using a massively parallel implementation of an evolutionary algorithm. Additionally, a frequency-fixing scheme is employed to deal with the constraint on the frequency of the fundamental mode. Finally, the computed Pareto front approximation and an RF cavity shape with desired properties are shown.

INTRODUCTION

Superconducting RF cavities are mainly optimized with respect to the properties of the fundamental mode [1]. However, in high current machines, such as the FCC-ee-Z [2], monopole and dipole modes are major sources of beam instability. The first monopole HOM band can be untrapped by enlarging the beam pipe radius, but the first dipole band remains trapped in the cavity and requires a special damping mechanism. In order to ease the HOM damping of the first dipole band, in this paper, a multi-objective shape optimization of a single-cell cavity that takes into account both the fundamental mode and the first dipole band is performed. The optimization algorithm is described on the concrete problem of optimizing the shape of the axisymmetric cavity for the FCC-ee-Z, but the same method can be used with other objectives and parameterizations.

MULTI-OBJECTIVE OPTIMIZATION

In this paper four objective functions have to be optimized simultaneously. First, the distance between the frequency of the first dipole mode, f_1 , which is typically the TE₁₁₁ mode, and the frequency of the fundamental mode, f_0 , has to be maximized. Second, the distance between f_1 and the frequency of the second dipole mode, f_2 , which is typically the TM₁₁₀ mode, has to be minimized. These two objectives simplify the design of the HOM couplers for damping the first dipole band. Third, the sum of the transverse shunt impedances of the dipole modes has to be minimized. The following definition of the transverse shunt impedance for

the dipole modes is used [3]

$$\frac{R}{Q_{\perp}} = \frac{(V_{||}(r=r_0) - V_{||}(r=0))^2}{k^2 r_0^2 \omega U},$$

where k is the wave number, r_0 the offset from the axis, ω the angular frequency, and U the stored energy. Fourth, $G_0 \cdot R/Q_0$ (G_0 is the geometry factor) of the fundamental mode has to be maximized, since it is inversely related to the dissipated power on the surface of the cavity [4]. In addition to these four objectives, f_0 has to be fixed to the operating frequency of 400.79 MHz.

Seven variables (R_{eq} , R_i , L , A , B , a and b) uniquely describe the shape of an elliptical cavity as shown in Fig. 1. The wall slope angle α can be computed from these design variables and, in order to avoid re-entrant shape cavities, it must be at least 90°.

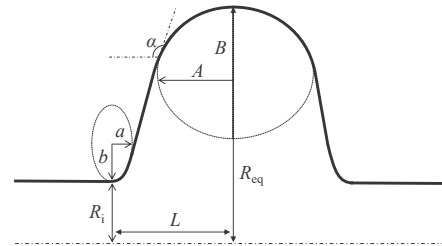


Figure 1: Parameterization of a single-cell elliptical cavity.

This can be formulated as the constrained multi-objective optimization problem

$$\begin{aligned} \min_{R_i, L, A, B, a, b} \quad & \underbrace{(f_0 - f_1)}_{F_1}, \underbrace{|f_1 - f_2|}_{F_2}, \underbrace{\frac{R}{Q_{\perp 1}} + \frac{R}{Q_{\perp 2}}}_{F_3}, \underbrace{-G_0 \cdot \frac{R}{Q_0}}_{F_4}, \\ \text{subject to} \quad & f_0 = 400.79 \text{ MHz and } \alpha \geq 90^\circ. \end{aligned} \quad (1)$$

Since in a single-cell cavity there is no restriction on the length $2L$ of the cell (because the particle only passes through one cell), and since this length highly affects f_1 , L is also taken to be a design variable. On the other hand, the variable R_{eq} has the highest influence on the value of f_0 , so it is not considered to be a design variable in the optimization, but rather used to tune f_0 to the desired value.

As part of the field leaks into the beam pipe, the cell and the beam pipe are simulated together and f_0 is tuned to 400.79 MHz taking the beam pipe effect into account. In this paper, the beam pipe length is set to the value of the wave length $\lambda = 748$ mm.

* marija.kranjcevic@inf.ethz.ch

FORWARD SOLVER

When solving time-harmonic Maxwell's equations in a vacuum axisymmetric RF cavity with perfectly electrically conducting (PEC) boundary conditions (BC) using the finite element method, one gets a generalized eigenvalue problem (GEVP) for each $m \in \mathbb{N}_0$ [5, 6]. The parameter m is the azimuthal mode number, and it is 0 for monopole modes, 1 for dipole modes, etc. Since the cross section of the single-cell elliptical cavity, as shown in Fig. 1, is symmetric, it is sufficient to solve time-harmonic Maxwell's equations in only half of it, once with PEC and once with perfectly magnetically conducting (PMC) BC on the symmetry plane.

For a specific value of R_{eq}, R_i, L, A, B, a and b , half of the cross section of the corresponding cavity is created and meshed. In order to compute the properties of the fundamental mode, the smallest eigenpair of the GEVP corresponding to $m = 0$ and PEC BC is found (TM₀₁₀). Similarly, to compute the properties of the dipole modes, the smallest eigenpair of the GEVPs corresponding to $m = 1$ and PEC (TM₁₁₀) and PMC (TE₁₁₁) BC on the cross section symmetry plane is found.

OPTIMIZATION ALGORITHM

Evolutionary Algorithm (EA)

A design point $\mathbf{d}_1 = (R_{i,1}, L_1, A_1, B_1, a_1, b_1)$ dominates \mathbf{d}_2 if it is not worse in any of the objectives, and it is strictly better in at least one objective. A massively parallel implementation of an EA [7], combined with the axisymmetric Maxwell eigensolver [8], is used to find points that are not dominated by any other point, called Pareto optimal points. The basic steps of an EA are given in Algorithm 1. The individuals (i.e., the RF cavities) comprising the first generation are chosen randomly, i.e., their design variable values are chosen randomly from a given interval (line 1). The values used in this paper are given in Table 1. These individuals are then evaluated, i.e., their objective function values are computed (line 2). After that, a predetermined number of cycles is performed, each resulting in a new generation (lines 3-7). In every cycle, crossover and mutation operators are used to create new individuals (lines 4-5) which are subsequently evaluated (line 6). The new generation is chosen to comprise approximately N fittest individuals (line 7).

Algorithm 1 Evolutionary algorithm

- 1: random population of individuals, $I_i, i = 1, \dots, N$
 - 2: evaluate the population
 - 3: **for** a predetermined number of generations **do**
 - 4: **for** pairs of individuals I_i, I_{i+1} **do**
 - 5: crossover(I_i, I_{i+1}), mutate(I_i), mutate(I_{i+1})
 - 6: evaluate new individuals
 - 7: choose N fittest individuals for the next generation
-

Table 1: Design Variable Bounds, in mm

Variable	R_i	L	A	B	a	b
Lower bound	145	120	40	40	10	10
Upper bound	160	190	140	140	70	70

Constraint Handling

For each design point $\mathbf{d} = (R_i, L, A, B, a, b)$ it is first necessary to determine the value of R_{eq} for which the frequency of the fundamental mode is $f_0 = 400.79$ MHz. This can be done with a zero-finding method. In this paper, TOMS 748 [9] is used, with the initial guess (in mm) $R_{eq} \in [325, 375]$. Furthermore, each time f_0 is computed for this fixed \mathbf{d} and a specific R_{eq} , it is enough to solve the eigenproblem corresponding to $m = 0$ and PEC BC, and, as long as f_0 is far away from the desired value, a coarse mesh can be used to speed up this process. If such a value of R_{eq} is not found, the individual is declared invalid and discarded from the population. Similarly, the individual is discarded if the value of the wall slope angle α is below 90° .

RESULTS

The optimizations were run on the Euler cluster¹ (Euler I and II) of ETH Zurich. The coarse eigensolves use a mesh with around 10'000 triangles, and the fine ones around 300'000 triangles. Solving just one coarse eigenproblem (meshing, computing 3 smallest eigenpairs and the objective function values) takes around 2 s. Solving a fine one takes around 90 s (24 s for meshing, 64 s for computing the eigenpairs, and 2 s for computing the objective function values). On average, 4 fine eigensolves are necessary to find the value of R_{eq} and the properties of the fundamental mode. After that, two more fine eigensolves (using an existing mesh) are needed to compute the properties of the dipole modes. Computing 50 generations of the EA with $N = 100$ (where almost 30% of the evaluated individuals get discarded from the optimization) using 96 processes takes around 13h.

The 50-th generation of an optimization with $N = 100$ is illustrated in Figs. 2 and 3. Each square represents an individual in the generation, i.e., an RF cavity shape. For all of these individuals $f_0 = 400.79$ MHz and $\alpha \geq 90$, i.e., both constraints from (1) are satisfied. In Fig. 2, the x and y coordinates represent the values of F_1 and F_3 , respectively, and the color shows the value of F_2 . The functions F_1 and F_3 are inversely correlated, and F_1 and F_2 do not seem to be conflicting, i.e., for lower values of F_1 , the values of F_2 are usually also lower. In Fig. 3, the x and y coordinates represent the values of F_2 and F_3 , respectively, and the value of F_4 is indicated by the color. The functions F_2 and F_3 are also inversely correlated.

The aperture radius R_i and the cell length $2L$ have a high impact on the objective functions. The value of f_1 is more sensitive to the changes in R_i and L than f_2 . If f_1 increases

¹ <https://scicomp.ethz.ch/wiki/Euler>

and gets closer to f_2 , both F_1 and F_2 improve (note that f_0 is fixed). A decrease in R_i typically increases f_1 , f_2 and $G_0 \cdot R/Q_0$, which improves F_1 , F_2 and F_4 , but also increases $R/Q_{\perp 1}$ and $R/Q_{\perp 2}$, so F_3 deteriorates. A decrease in L , on the other hand, decreases $G_0 \cdot R/Q_0$ and $R/Q_{\perp 1}$, and increases f_1 and $R/Q_{\perp 2}$ (which is typically much larger than $R/Q_{\perp 1}$). Therefore, there is an inverse correlation between the sum of the impedances of the first dipole band (F_3) and their frequency difference (F_2 and F_1). The x axis in Fig. 3 is a reshuffled version of the x axis in Fig. 2, based on f_2 . Since both L and R_i have a high influence on f_1 and only L highly impacts f_2 , these two variables do not always move in the same direction and a wiggly behavior is observed in the Pareto front approximation (orange line) in Fig. 3.

The values of design variables and objective functions for a chosen individual are given in Table 2. Note that the design variables are allowed to go outside of the specified bounds if it helps to improve the objective functions. Some additional information is given in Table 3, and the shape of the RF cavity is shown in Fig. 4.

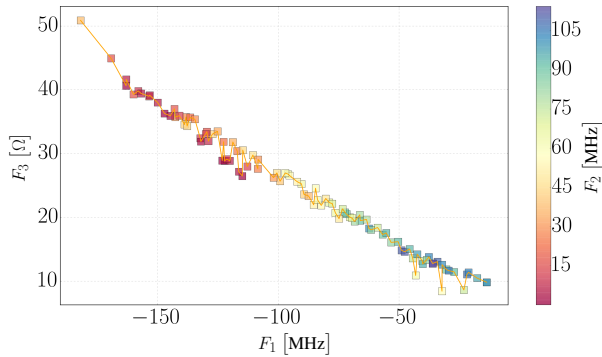


Figure 2: The relationship between F_1 , F_2 and F_3 for the individuals in the 50-th generation of the EA.

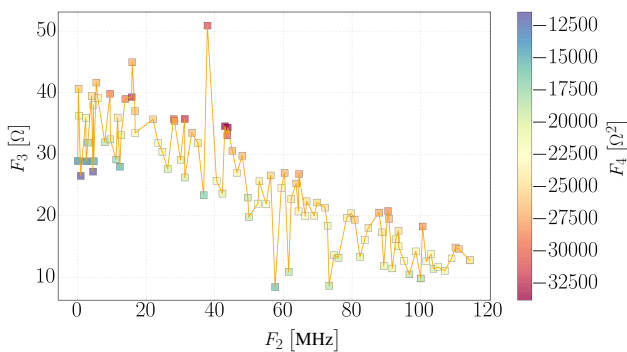


Figure 3: The relationship between F_2 , F_3 and F_4 for the individuals in the 50-th generation of the EA.

CONCLUSIONS

In this paper an optimization algorithm for solving constrained multi-objective shape optimization problems for RF cavities was proposed and applied to the problem of optimizing the shape of the superconducting RF cavity for the FCC-ee-Z with respect to both the fundamental mode



Figure 4: The electric field of the fundamental mode in half of the chosen RF cavity.

Table 2: Description of the Chosen RF Cavity

Variable	R_i [mm]	L [mm]	A [mm]	B [mm]
Value	141.614	146.270	103.54	127.521
Variable	a [mm]	b [mm]	R_{eq} [mm]	α [°]
Value	41.921	45.812	339.166	91.697
Objective	F_1 [MHz]	F_2 [MHz]	F_3 [Ω]	F_4 [Ω ²]
Value	-147.03	0.40	36.3	-2.13e3

Table 3: Additional Information on the Chosen RF Cavity

TM₀₁₀	$f_0 = 400.79$ MHz	$\frac{R}{Q_0} = 94.9$ Ω
	$\frac{E_{pk}}{E_{acc}} = 1.92$	$\frac{B_{pk}}{E_{acc}} = 4.16$ $\frac{\text{mT}}{\text{MV/m}}$
TE₁₁₁	$f_1 = 547.82$ MHz	$\frac{R}{Q_{\perp 1}} = 5.10$ Ω
TM₁₁₀	$f_2 = 548.22$ MHz	$\frac{R}{Q_{\perp 2}} = 31.2$ Ω

and the first dipole band. The proposed algorithm and its implementation could be used to optimize the shape of other axisymmetric RF structures, taking into account also the HOMs corresponding to arbitrary azimuthal mode numbers.

ACKNOWLEDGEMENTS

This research was supported by the German Research Foundation (Deutsche Forschungsgemeinschaft, DFG) within the project RI 814/29-1. The computations were executed on the Euler compute cluster of ETH Zurich at the expense of a Paul Scherrer Institut (PSI) grant.

REFERENCES

- [1] V. Shemelin, S. Gorgi Zadeh, J. Heller, and U. van Rienen, “Systematical study on superconducting radio frequency elliptic cavity shapes applicable to future high energy accelerators and energy recovery linacs”, *Phys. Rev. Accel. Beams*, vol. 19, 2016. doi:10.1103/PhysRevAccelBeams.19.102002
- [2] S. Gorgi Zadeh, R. Calag, F. Gerigk, and U. van Rienen, “FCC-ee Hybrid RF Scheme”, in *Proc. IPAC’18*, Vancouver, BC, Canada, Apr-May 2018. doi:10.18429/JACoW-IPAC2018-MOPMF036
- [3] B. P. Xiao *et al.*, “Higher Order Mode Filter Design for Double Quarter Wave Crab Cavity for the LHC High Luminosity Upgrade”, in *Proc. IPAC’15*, Richmond, VA, USA, May 2015. doi:10.18429/JACoW-IPAC2015-WEPWI059

- Content from this work may be used under the terms of the CC BY 3.0 licence (© 2018). Any distribution of this work must maintain attribution to the author(s), title of the work, publisher, and DOI.
- [4] J. Sekutowicz *et al.*, “Cavities for JLAB’s 12 GeV Upgrade”, in *Proc. PAC’03*, Portland, OR, USA, May 2003, paper TPAB085. <http://jacow.org/p03/PAPERS/TPAB085.PDF> and doi: 10.1109/PAC.2003.1289717
 - [5] P. Arbenz and O. Chinellato, “On solving complex-symmetric eigenvalue problems arising in the design of axisymmetric VCSEL devices”, *Appl. Numer. Math.*, vol. 58, no. 4, pp. 381-394, 2008. doi: 10.1016/j.apnum.2007.01.019
 - [6] O. Chinellato, “The complex-symmetric Jacobi–Davidson algorithm and its application to the computation of some resonance frequencies of anisotropic lossy axisymmetric cavities”, ETH Zurich, Diss. ETH No. 16243, 2005.
 - [7] Y. Ineichen *et al.*, “A fast and scalable low dimensional solver for charged particle dynamics in large particle accelerators”, *Comput. Sci. Res. Dev.*, vol. 28, no. 2, pp. 185-192, 2013. doi:10.1007/s00450-012-0216-2
 - [8] M. Kranjčević, A. Adelman, P. Arbenz, A. Citterio, and L. Stingelin, “Multi-objective shape optimization of radio frequency cavities using an evolutionary algorithm”, ArXiv e-prints, 2018. arXiv:1810.02990
 - [9] G. E. Alefeld, F. A. Potra, and Y. Shi, “Algorithm 748: Enclosing Zeros of Continuous Functions”, *ACM Trans. Math. Softw.*, vol. 21, no. 3, pp. 327-344, 1995. doi:10.1145/210089.210111